2009 American Control Conference
Hyatt Regency Riverfront, St. Louis, MO, USA
June 10-12, 2009

Departure Resilient Control for Autonomous Air Vehicles

James A. Ramsey, Ryan T. Ratliff, Kevin A. Wise
The Boeing Company
St. Louis, MO, USA
james.a.ramsey@boeing.com

Eugene Lavretsky
The Boeing Company
Huntington Beach, CA, USA

***Abstract*— A new approach for developing guidance and control laws for aircraft that have departed controlled flight is presented. The method leverages and produces flight trajectories similar to what pilots would perform. The method induces a periodic orbit and then escapes from the periodic orbit into normal flight. The problem is approached from the inertial reference frame in order to better define the behavior of periodic orbit dynamics. A control law that effectively maps the aircraft inertial dynamics to bifurcations facilitates the production of periodic orbit behavior. In addition to circular orbits, the control law proves to expand the set to elliptical orbits and presents a framework for alternative orbit geometries.**

I. Introduction

Current and future missions for modern unmanned aircraft are requiring smaller, lighter, and more flexible designs. In addition to the inherent challenges exacerbated by these designs in the normal operating envelope, there will also be greater susceptability to departure resulting from environmental disturbances like gusts and wind shears that exceed the predescribed control authority. This is considered uncommanded departure. There could also be cases where departed flight is commanded. For example, consider a small micro air vehicle (MAV) parked on the edge of an urban structure as illustrated in Figure 1. It

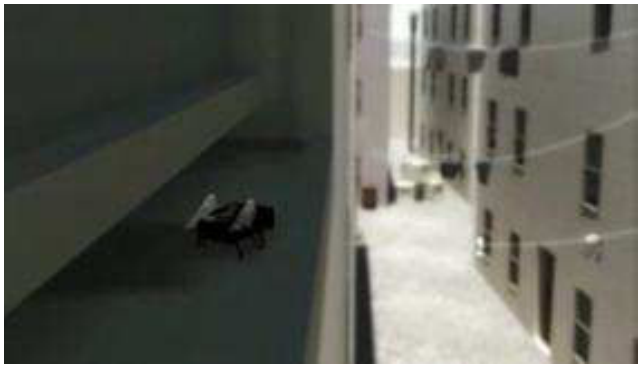

Fig. 1. MAV launching into a departed flight condition

is desirable to launch the MAV from the structure and proceed into normal flight. However, the instantaneous condition of the MAV upon separation from the building is departed flight. A procedure is required to transition the MAV from the departed state to normal flight. Another case, depicted in Figure 2, consists of an aircraft landing between two tall obstacles with a short runway. A conventional

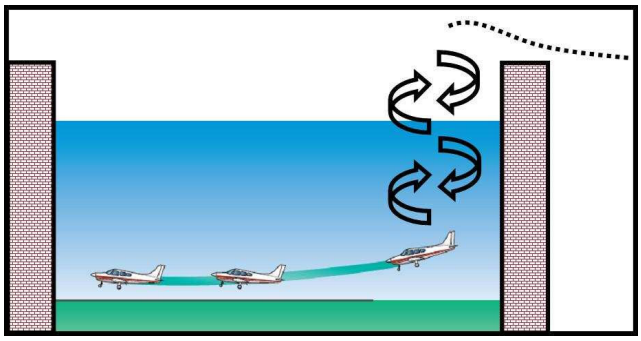

Fig. 2. Short runway landing with constraints

landing would normally require a steep descent. However, deliberately departing the aircraft from normal flight and invoking a recovery procedure adds an alternative landing strategy that reduces the airspeed and flight path angle on approach. These procedures will require the aircraft to maneuver through brief periods of unstable and/or uncontrollable flight. Therefore, flight control architectures for these aircraft will need to accommodate these conditions and continue the desired mission. Unmanned aircraft with this capability will demonstrate improved mission reliability, survivability, and effectiveness.

Departure from normal flight typically occurs when an aircraft wing *stalls* or exceeds some local angle-of-attack (AOA) threshold. Upon stall, some aircraft are configured such that the lift force provides a centripetal acceleration to balance an angular velocity inducing a stable periodic orbit or *spin* [1]. Altitude loss accompanies the periodic orbits and, therefore, escaping from these equilibria is necessary to prevent ground impact. As previously mentioned, the sequence of departure and recovery behavior can be beneficial in certain scenarios, and the ability to command and track induction and escape maneuvers can be advantageous to mission reliability. In flying manned aircraft, recovery from spins (and flat spins) requires moving control surfaces in non-intuitive directions, generally speeding up the descent in order to increase airflow over the control surfaces, reinstate control, and subsequently pull up into level flight.

Previous research in spin recovery techniques has primarily focused on inner-loop or body rate dynamics and control. An investigation into the relationship between the magnitude of body moments and number of spin turns was conducted to determine the amount of control required for

978-1-4244-4524-0/09/$25.00 ©2009 AACC

satisfactory recovery [2]. Stall/spin prediction and identification was investigated in [1], [3] where numerical and graphical techniques were used to identify flight conditions indicative of spin induction for a given aircraft. Multiple inner-loop, feedback linearization flight control laws were designed in [4]. One control law instigates the aircraft into a periodic orbit subsequent to stall while the second brings the aircraft back to the normal flight regime after escaping the orbit. Optimization techniques are used in [5] to provide necessary conditions for spin recovery while simultaneously minimizing altitude loss.

This research, however, analyzes departure resilience in the inertial navigation frame. The primary advantage is that it allows not only analysis and control of the *instigation* of departure induction and recovery, but also the *behavior*. Furthermore, the inertial frame provides analytic solutions which will be exploited using bifurcation theory. Control solutions can be implemented in an outer-loop, guidance law potentially requiring only a single inner-loop autopilot. Changes in the induction and recovery process and behavior can be reflected in the guidance law and mapped to the autopilot. This proves to reduce complexity in the analysis, design and implementation.

II. Modeling

Aircraft departure from and reinstatement to normal flight is assumed to occur in small regions over the earth surface. Therfore, coriolis forces from the earth's curvature can be neglected and a flat-earth approximation can be used. The three degree of freedom, flat-earth navigation dynamics can be representned by [6]

$$\dot{x} = V\cos\chi\cos\gamma \tag{1}$$
$$\dot{y} = V\sin\chi\cos\gamma \tag{2}$$
$$\dot{h} = V\sin\gamma \tag{3}$$
$$\dot{V} = -g\sin\gamma + u_V \tag{4}$$
$$\dot{\chi} = \frac{u_\chi}{V\cos\gamma} \tag{5}$$
$$\dot{\gamma} = \frac{u_\gamma - g\cos\gamma}{V} \tag{6}$$

where coordinates x and y and the altitude h specify the position of the center of gravity of the aircraft in an earth-based reference frame. The orientation of the aircraft velocity vector is denoted by the heading angle, χ, and flight path angle, γ. The heading angle is the angle between the projection of the velocity vector onto the xy plane and the x-axis. The angle between the velocity vector and its projection onto the xy plane is the flight path angle. The aircraft velocity V is assumed to be equal to the airspeed and g is the acceleration due to gravity. The guidance loop control variables u_V, u_γ, u_χ are inertial accelerations related to the axial thrust, T, lift force, L, and side force C, respectively. The controls must be designed to influence a desired airspeed and direction.

A. Bifurcation Analysis

As discussed in Section I, some aircraft are configured to induce a periodic orbit or *spin* while descending after normal flight departure. With appropriate control authority, the orbit can then actually be used to return the aircraft to normal flight. This procedure of sequentially transitioning an aircraft through a point of instability, to a stable periodic orbit, and back to stable normal flight is charateristic of a bifurcating system. Specifically, the Hopf bifurcation [7] provides a legitimate candidate to model the behavior of an aircraft through a departure induction and recovery procedure. The normal form of the Hopf bifurcation is

$$\dot{v}_x = v_x\left(\mu - \lambda v_x^2 - \lambda v_y^2\right) - \zeta v_y \tag{7}$$
$$\dot{v}_y = v_y\left(\mu - \lambda v_x^2 - \lambda v_y^2\right) + \zeta v_x \tag{8}$$

where the variables v_x and v_y represent velocity components in x and y, respectively, μ is the bifurcation parameter and λ is the first Lyapunov quantity. The rate at which the system travels along a trajectory is controlled by ζ. When $\lambda > 0$ and μ changes from negative to positive, a locally stable focus bifurcates into a globally attractive periodic orbit. The resulting stable configuration is known as a *supercritical* state and characterizes an aircaft transition into a stable spin. Conversely, when μ changes from positive to negative, a *subcritical* transition occurs whereby the globally stable periodic orbit collapses to a locally stable equilibrium point at the origin. This is representative of aircraft spin recovery back to a normal mode of operation. When $\lambda < 0$ and $\mu > 0$ only an unstable focus is created at the origin. However, when $\mu, \lambda < 0$, an invariant unstable periodic orbit exists which surrounds a locally stable focus at the origin. It is important to note that the bifurcation parameters need not be constant. In certain cases it becomes advantageous for μ and λ to be functions of the state variables as will be illustrated in Section IV.

B. Elliptical Orbits

One advantage of using an outer-loop, inerital frame approach to departure resilience analysis is that insights into the trajectory geometric behavior can be extracted. This frame is natural in that system requirements for manueuvering are easily specified, and instances where the trajectory tracks a predetermined, mathematically defined shape or geometric contour may be desirable. For example, spatial constraints may restrict an aircraft from achieving a circular periodic orbit. However, there may be other geometric shapes or contours the vehicle can track which satisfy the constraints. Additionally, some aircraft configurations may not be capable of achieving a circular periodic orbit equilibria at a given flight condition for a given set of controls. However, geometrically non-circular periodic orbits may be achievable. The following discussion presents a modification of the Hopf bifurcation normal form such that the induced periodic orbit takes and elliptical shape in the inertial velocity phase plane.

Equations (7) and (8) represent circular (symmetric) periodic orbits. Another form of the Hopf bifurcation producing an elliptical (asymmetric) orbit can be found by splitting the single parameter λ into λ_1 and λ_2 where $\lambda_1 \neq \lambda_2$. This results in

$$\dot{v}_x = v_x\left(\mu - \lambda_1 v_x^2 - \lambda_2 v_y^2\right) - \zeta v_y \tag{9}$$
$$\dot{v}_y = v_y\left(\mu - \lambda_1 v_x^2 - \lambda_2 v_y^2\right) + \zeta v_x \tag{10}$$

Necessary and sufficient conditions for (9) and (10) to satisfy an invariant elliptical orbit centered about the origin are that the trajectories satisfy the general equation of an ellipse

$$E(v_x, v_y) = Av_x^2 + Bv_xv_y + Cv_y^2 = 1 \tag{11}$$

where $B^2 < 4AC$ for some constants A, B, C and

$$\frac{dE(v_x, v_y)}{dt}\,|_{\{Av_x^2+Bv_xv_y+Cv_y^2=1\}} = 0 \tag{12}$$

Differentiating (11) gives

$$\begin{aligned}\frac{dE(v_x, v_y)}{dt} &= 2Av_x\dot{v}_x + B\dot{v}_xv_y + Bv_x\dot{v}_y + 2Cv_y\dot{v}_y \\ &= 2(Av_x^2 + Bv_xv_y + Cv_y^2)(\mu + \lambda_1 v_x^2 + \lambda_2 v_y^2) \\ &\quad + 2(A-C)\zeta v_xv_y + B\zeta v_y^2 - B\zeta v_x^2\end{aligned}$$

Substituting (11), collecting terms, and negating results in

$$\begin{aligned}-\frac{dE(v_x, v_y)}{dt} &= -2\mu - (-B\zeta - 2\lambda_1)v_x^2 - (B\zeta - 2\lambda_2)v_y^2 \\ &\quad - 2(A-C)\zeta v_xv_y\end{aligned} \tag{13}$$

Multiplying (11) by $k > 0$, rewriting and equating to (13) produces

$$\begin{aligned}&kAv_x^2 + kBv_xv_y + kCv_y^2 - k \\ &\quad = -2\mu - (-B\zeta - 2\lambda_1)v_x^2 - 2(A-C)\zeta v_xv_y \\ &\qquad - (B\zeta - 2\lambda_2)v_y^2\end{aligned} \tag{14}$$

Therefore, matching coefficients in (14) results in the following restrictions

$$\begin{aligned}kA &= B\zeta + 2\lambda_1 \\ kB &= -2(A-C)\zeta \\ kC &= -B\zeta + 2\lambda_2 \\ k &= 2\mu\end{aligned}$$

Solving for A,B, and C gives the solution set

$$\begin{aligned}A &= \frac{\zeta^2(\lambda_1+\lambda_2) + 2\lambda_1\mu^2}{2\mu(\zeta^2+\mu^2)} \\ B &= -\frac{\zeta(\lambda_2-\lambda_1)}{\zeta^2+\mu^2} \\ C &= \frac{\zeta^2(\lambda_1+\lambda_2) + 2\lambda_2\mu^2}{2\mu(\zeta^2+\mu^2)}\end{aligned} \tag{15}$$

for which (11) and (12) are satisfied. Ensuring that $B^2 < 4AC$ requires

$$\frac{\zeta^2(\lambda_1+\lambda_2)^2 + 4\lambda_1\lambda_2\mu^2}{(\zeta^2+\mu^2)\mu^2} > 0 \tag{16}$$

It is desirable to map the bifurcation parameters to the geometric parameters of an ellipse. The geometric representation of an ellipse in *standard position* centered at the origin and rotated by some angle δ relative to the x-axis can be described mathematically by

$$\frac{(v_x\cos\delta + v_y\sin\delta)^2}{a^2} + \frac{(v_y\cos\delta - v_x\sin\delta)^2}{b^2} = 1 \tag{17}$$

where $\max(a,b)$ is the semi-major axis and $\min(a,b)$ is the semi-minor axis. Collecting terms in v_x and v_y of (17) gives

$$\begin{aligned}&\left(\frac{b^2\cos^2\delta + a^2\sin^2\delta}{a^2b^2}\right)v_x^2 + \left(\frac{2(b^2-a^2)\sin\delta\cos\delta}{a^2b^2}\right)v_xv_y \\ &\quad + \left(\frac{a^2\cos^2\delta + b^2\sin^2\delta}{a^2b^2}\right)v_y^2 = 1\end{aligned} \tag{18}$$

Comparing coefficients in (11) and (18) and using (15) to solve in terms of the bifurcation parameters gives

$$\frac{\lambda_1}{\mu} = \frac{(a^2+b^2)\cos^2\delta - a^2}{a^2b^2(2\cos^2\delta - 1)} \tag{19}$$
$$\frac{\lambda_2}{\mu} = \frac{(a^2+b^2)\cos^2\delta - b^2}{a^2b^2(2\cos^2\delta - 1)} \tag{20}$$
$$\frac{\zeta}{\mu} = \frac{2\sin\delta\cos\delta}{2\cos^2\delta - 1} \tag{21}$$

Therefore, given any geometric representation of an ellipse that describes desireable aircraft behavior, the mapping (19)-(21) defines the necessary bifurcation parameters. Note that (19)-(21) demonstrates that the invariant elliptical orbit must have a nonzero rotation angle with respect to the x-axis. Otherwise, B will be zero and invariance will no longer hold.

III. Control Design

This section describes candidate guidance laws that will produce Hopf bifurcation inducing commands to a body axis, inner-loop flight control system. Differentiating (1) and (2) and noting that $\dot{x} = v_x$ and $\dot{y} = v_y$ gives

$$\dot{v}_x = (\dot{V}\cos\chi - V\sin\chi\dot{\chi})\cos\gamma - V\cos\chi\sin\gamma\dot{\gamma} \tag{22}$$
$$\dot{v}_y = (\dot{V}\sin\chi + V\cos\chi\dot{\chi})\cos\gamma - V\sin\chi\sin\gamma\dot{\gamma} \tag{23}$$

Substituting (4), (5),and (6) into (22) and (23) results in

$$\begin{aligned}\dot{v}_x &= (-g\sin\gamma + u_V)\cos\chi\cos\gamma - \sin\chi\,u_\chi \\ &\quad - \cos\chi\sin\gamma(u_\gamma - g\cos\gamma) \\ &= (-g\sin\gamma + u_V)\frac{\dot{x}}{V} - \sin\chi\,u_\chi \\ &\quad - \cos\chi\sin\gamma(u_\gamma - g\cos\gamma)\end{aligned} \tag{24}$$

$$\begin{aligned}\dot{v}_y &= (-g\sin\gamma + u_V)\sin\chi\cos\gamma + \cos\chi\,u_\chi \\ &\quad - \sin\chi\sin\gamma(u_\gamma - g\cos\gamma) \\ &= (-g\sin\gamma + u_V)\frac{\dot{y}}{V} + \cos\chi\,u_\chi \\ &\quad - \sin\chi\sin\gamma(u_\gamma - g\cos\gamma)\end{aligned} \tag{25}$$

Choosing the state variables as $[x\ v_x\ y\ v_y\ V\ \chi\ \gamma]$ results in

$$\dot{x} = v_x \tag{26}$$

$$\dot{v}_x = (-g\sin\gamma + u_V)\frac{v_x}{V} - \sin\chi\, u_\chi - \cos\chi\sin\gamma(u_\gamma - g\cos\gamma) \tag{27}$$

$$\dot{y} = v_y \tag{28}$$

$$\dot{v}_y = (-g\sin\gamma + u_V)\frac{v_y}{V} + \cos\chi\, u_\chi - \sin\chi\sin\gamma(u_\gamma - g\cos\gamma) \tag{29}$$

Now the control variables u_V, u_χ, u_γ, need to be chosen such that a Hopf bifurcation of the navigational position states results. Choosing the control variables as

$$u_V = g\sin\gamma + V(\mu - \lambda_1 v_x^2 - \lambda_2 v_y^2) \tag{30}$$

$$u_\chi = \zeta V\cos\gamma \tag{31}$$

$$u_\gamma = g\cos\gamma \tag{32}$$

will result in the Hopf bifurcation system of (7) and (8). The guidance laws required to instantiate the Hopf bifurcation are not unique. For example, another option that emphasizes the flight path angle variable, u_γ, for bifurcation control rather than the airspeed is

$$u_V = g\sin\gamma \tag{33}$$

$$u_\chi = \zeta V\cos\gamma \tag{34}$$

$$u_\gamma = g\cos\gamma - V\cot\gamma(\mu - \lambda_1 v_x^2 - \lambda_2 v_y^2) \tag{35}$$

Note that although the $\cot\gamma$ term in (35) induces a singular solution at $\gamma = 0$, this state is not indicative of an aircraft in flat spin mode. During the spin, the aircraft will be descending rapidly at a large AOA and the flight path angles are typically in the range of $\frac{\pi}{3} < \gamma < \frac{\pi}{2}$. Substituting the controls (33)-(35) into the aircraft navigation equations results in the closed-loop system

$$\begin{aligned}
\dot{x} &= v_x \\
\dot{v}_x &= v_x\left(\mu - \lambda_1 v_x^2 - \lambda_2 v_y^2\right) - \zeta v_y \\
\dot{y} &= v_y \\
\dot{v}_y &= v_y\left(\mu - \lambda_1 v_x^2 - \lambda_2 v_y^2\right) + \zeta v_x \\
\dot{h} &= V\sin\gamma \\
\dot{V} &= 0 \\
\dot{\chi} &= \zeta \\
\dot{\gamma} &= -\cot\gamma(\mu - \lambda_1 v_x^2 - \lambda_2 v_y^2)
\end{aligned}$$

The velocity states, v_x, v_y, behave as desired from (9) and (10). Airspeed is maintained ($\dot{V} = 0$) using u_v, and the heading rate, $\dot{\chi}$, is equivalent to the speed of the elliptical orbit, ζ, as expected.

The inertial frame control variables must be mapped to a flight control law in body or wind frame control variables. The control variables u_γ, u_χ, u_V are directly related to the required inertial accelerations. An appropriate mapping can be applied to transform the inertial acceleration commands into the aircraft body frame acceleration commands. The body frame acceleration commands can then be injected into an inner-loop flight control law to produce the desired inertial reference bifurcating system.

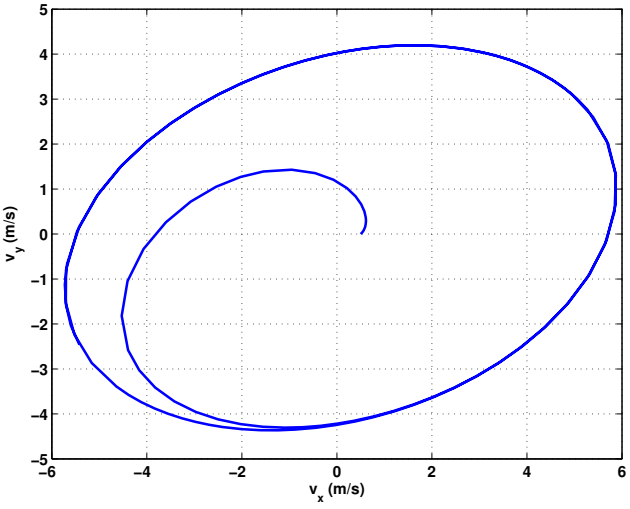

Fig. 3. Aircraft incipient orbit velocity phase plane

IV. Simulation Results

Simulations were conducted to verify the control design developed in the previous section. It is assumed the aircraft is in a post-stall state descending toward the earth surface. The simulation initial conditions are given in Table I. As the aircraft descends, control law (33)-(35) is implemented to insigate an elliptical periodic orbit and induce a supercritical Hopf bifurcation in the inertial velocity phase plane. The fully developed elliptical geometric properites were chosen as

TABLE I
Initial Conditions

Parameter	Value
x_0 (m)	0
v_{x0} ($\frac{\text{m}}{\text{sec}}$)	0.5
y_0 (m)	0
v_{y0} ($\frac{\text{m}}{\text{sec}}$)	0
h_0 (m)	3000
V_0 ($\frac{\text{m}}{\text{sec}}$)	20
χ_0 (deg)	0
γ_0 (deg)	-89

$$a = 6\,\frac{\text{m}}{\text{sec}}, \quad b = 4\,\frac{\text{m}}{\text{sec}}, \quad \delta = 20^\circ \tag{36}$$

for the semi-major axis, semi-minor axis, and rotation angle, respectively. Using (19)-(21) and arbitrarily choosing $\mu = 2$, gives

$$\lambda_1 = 0.045, \quad \lambda_2 = 0.136, \quad \zeta = 1.68$$

Figure 3 shows the orbit inception in the velocity phase plane verifying the desired elliptical geometric properties

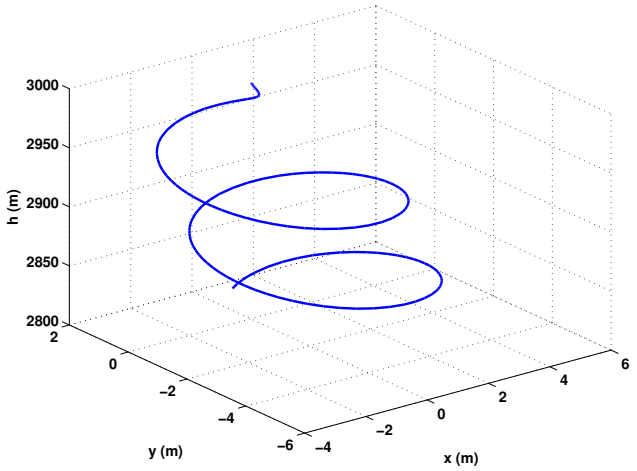

Fig. 4. Aircraft incipient orbit inertial coordinate trajectory

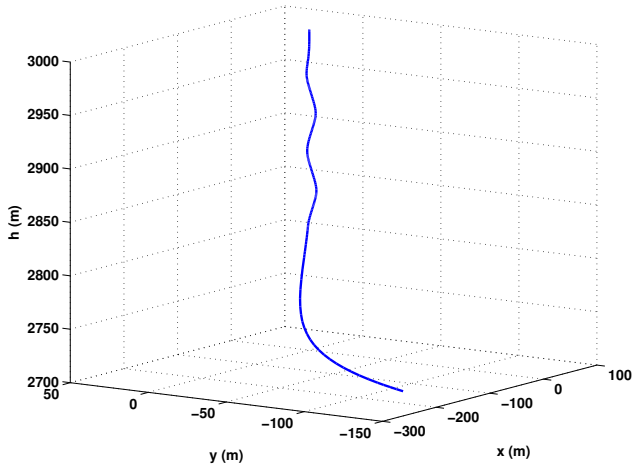

Fig. 5. Aircraft inertial coordinate trajectory

of (36). The rate at which the fully developed orbit is achieved can be increased (decreased) by increasing (decreasing) the value of μ. This will, obviously, effect control power generation requirements. The inertial frame orbit induction is illustrated in Figure 4.

As indicated in Section II, selecting the bifurcation variables as a function of the states can provide beneficial results. In this case, $\mu, \lambda_1, \lambda_2$ are selected as a function of flight path angle to compensate for the singularity as $\gamma \to 0$. After approximately 9.7 seconds, the bifurcation parameters of (35) are modified to functions of the flight path angle

$$\mu(\gamma) = 0.2\,\gamma\tan(\gamma) \quad \zeta = 0.05$$
$$\lambda_1(\gamma) = -10^{-4}\,\gamma\tan(\gamma) \quad \lambda_2(\gamma) = -10^{-4}\,\gamma\tan(\gamma)$$

where the sign reversal on λ_1, λ_2 destabilizes the periodic orbit about the origin while simultaneously collapsing the flight path angle and returning the aircraft to normal flight. The flight path angle closed-loop dynamics now become

$$\dot{\gamma} = -10^{-4}\,\gamma(200 + v_x^2 + v_y^2) \tag{37}$$

which exhibit exponential convergence characteristics and eliminate the Hopf bifurcation dynamics as the aircraft returns to normal flight ($\gamma \to 0$). The inertial space trajectory through orbit induction, development, and escape is shown in Figure 5. The aircraft descends approximately 200 meters in orbit and completes 2 full revolutions prior to the escape sequence. The radius of the orbit varies between 2 and 3 meters. The velocity phase plane, shown in Figure 6, depicts the propogation of the velocity direction where the heading stabilizes at around $-80°$ during the flight path angle collapse (Fig. 7). Generally, the maneuver control power requirements must be within the aircraft limits at the cooresponding range of flight conditions. For the selected elliptical geometry, the control accelerations remained within $12.2\,\frac{\text{m}}{\text{sec}^2}$ (1.25g) as shown in Figure 8. Naturally, increasing the magnitude of the elliptical geometry will increase the control power requirements. The magnitudes of the semi-major and semi-minor axis were doubled to $a = 12$ and

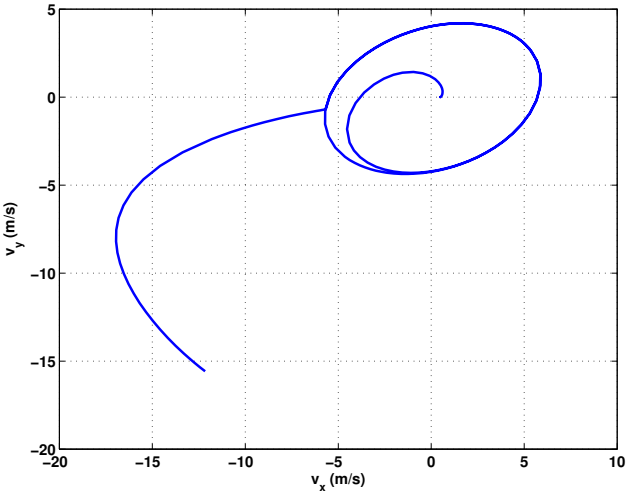

Fig. 6. Aircraft trajectory velocity phase plane

$b = 8$, respectively. Although u_γ and u_χ both increased, The controls did not double proportionally in magnitude. The control u_V remained approximately the same. The differences can be seen graphically in Figures 9 and 10 for the velocity phase plane and control power, respectively.

V. Conclusion

A recovery method was developed for autonomous air vehicles that have departed from normal flight. The method leverages techniques from piloted aircraft by inducing and escaping from periodic orbits subsequent to departure. Bifurcations are used to facilitate the production and define the behavior of aircraft departure recovery dynamics in the inertial reference frame. A control law is designed that effectively maps the aircraft inertial dynamics to the desired bifurcation behavior. Additionally, the set of periodic orbits is expanded beyond circular to include elliptical geometries. Invariant set theory is used to prove existence and stability of the elliptical orbits and presents a framework for alternative orbit geometries. Simulations were conducted to verify

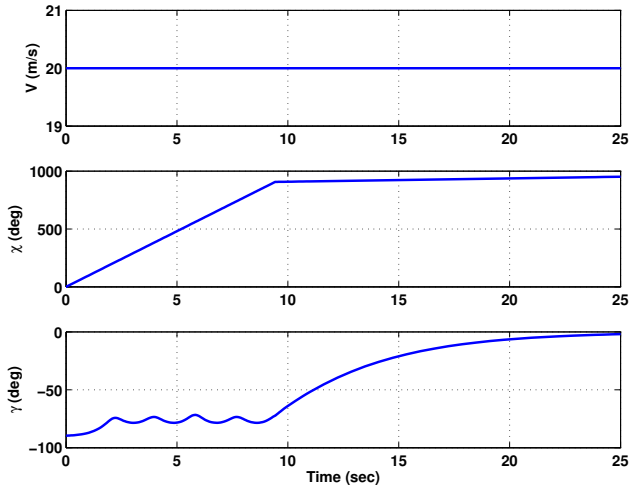

Fig. 7. Aircraft airspeed and inertial frame angles

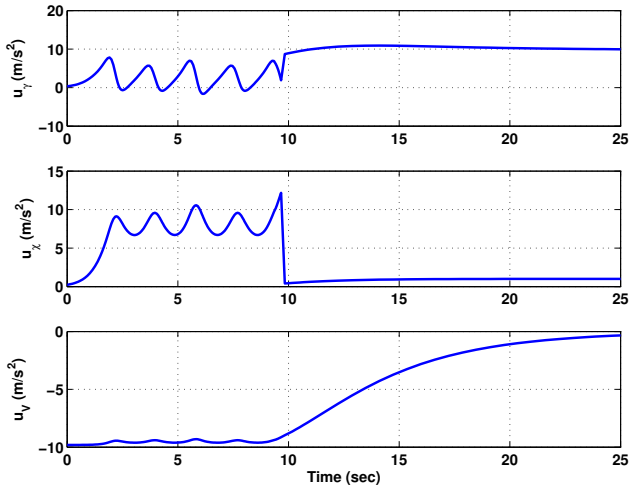

Fig. 8. Control trajectory

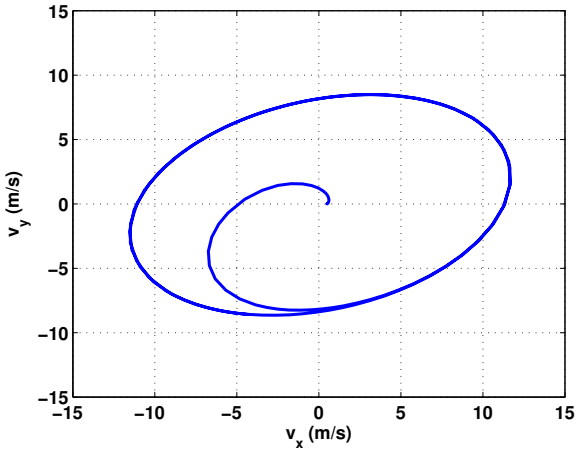

Fig. 9. Incipient orbit velocity phase plane ($a = 12, b = 8$)

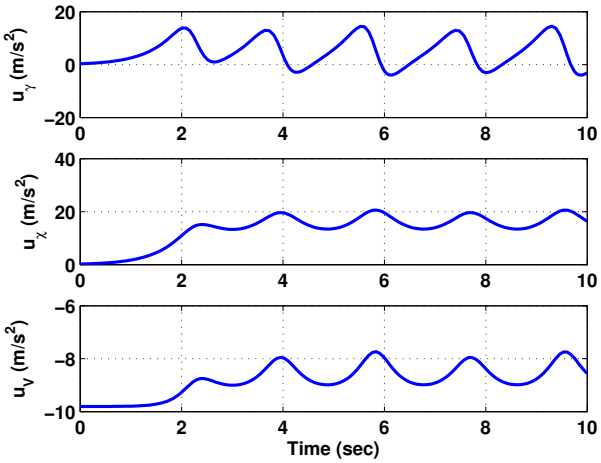

Fig. 10. Control trajectory ($a = 12, b = 8$)

the mathematical results.

Future work will focus on the six-degree-of-freedom aircraft body reference frame response to the corresponding inertial commanded laws developed in this work. The aircraft body reference frame analysis is expected to provide insight into the design and synthesis of inner-loop flight control laws. Furthermore, an effort will focus on configuration options that potentially provide built-in departure resilient capability without the use of a dedicated control algorithm. Also, alternative orbit geometries will be investigated for potential advantages in selected mission scenarios.

VI. Acknowledgement

This work was sponsored in part by the Air Force Office of Scientific Research, USAF, under grant/contract number FA9550-07-C-0051. The views and conclusions contained herein are those of the authors and should not be interpreted as necessarily representing the official policies or endorsements, either expressed or implied, of the Air Force Office of Scientific Research or the U.S. Government. The authors would like to thank Professor Chris Byrnes for many useful discussions

References

[1] M. B. Tischler and J. B. Barlow, "Dynamic analysis of the flat spin mode of a general aviation aircraft," *Journal of Aircraft*, vol. 19, no. 3, pp. 198–205, 1982.

[2] E. L. Anglin, "Relationship between magnitude of applied spin recovery moment and ensuing number of recovery turns," NASA, Tech. Rep. TN D-4077, August 1967.

[3] W. Bihrle and B. Barnhart, "Spin prediction techniques," *Journal of Aircraft*, vol. 20, no. 2, pp. 97–101, 1983.

[4] A. Saraf and G. Deodhare, "A feedback linearisation based nonlinear controller synthesis to recover an unstable aircraft from post-stall regime," AIAA-98-4206.

[5] G. R. Walsh, "Optimal spin recovery," *Journal of Engineering Mathematics*, vol. 3, no. 4, pp. 313–324, 1969.

[6] P. K. A. Menon, "Short-range nonlinear feedback strategies for aircraft pursuit-evasion," *Journal of Guidance*, vol. 12, no. 1, pp. 27–32, 1989.

[7] J. Guckenheimer and P. Holmes, *Nonlinear Oscillations, Dynamical Systems, and Bifurcations of Vector Fields*, 3rd ed. New York: Springer-Verlag, 1997.